

©2022. American Chemical Society. This manuscript version is made available under the CC-BY-NC-ND 4.0 license <http://creativecommons.org/licenses/by-nc-nd/4.0/>

**This item is the archived peer-reviewed author-version of:  
Engineering Aspects for the Design of a Bicarbonate Zero-Gap Flow Electrolyzer for the Conversion of CO<sub>2</sub> to Formate**

**Reference:**

Gutiérrez-Sánchez, O., De Mot, B., Bulut, M., Pant, D. and Breugelmans, T., 2022. Engineering Aspects for the Design of a Bicarbonate Zero-Gap Flow Electrolyzer for the Conversion of CO<sub>2</sub> to Formate. **ACS Applied Materials & Interfaces**, 14(27), pp.30760-30771.

ISSN 1944-8252 (2022), Copyright © 2022 American Chemical Society. All rights reserved

Full text (Publisher's DOI): <https://doi.org/10.1021/acsami.2c05457>

Received 28 March 2022; Received in revised form 15 May 2022; Accepted 17 June 2022

# Engineering Aspects for the Design of a Bicarbonate Zero-Gap Flow Electrolyzer for the Conversion of CO<sub>2</sub> to Formate

Oriol Gutiérrez-Sánchez<sup>a,b,1</sup>, Bert de Mot<sup>a,1</sup>, Metin Bulut<sup>b</sup>, Deepak Pant<sup>b,c</sup> and Tom Breugelmans<sup>\*a,c</sup>

<sup>a</sup> University of Antwerp, Research Group Applied Electrochemistry and Catalysis (ELCAT), Universiteitsplein 1, 2610 Wilrijk, Belgium.

<sup>b</sup> Separation and Conversion Technology, Flemish Institute for Technological Research (VITO), Boeretang 200, Mol 2400, Belgium.

<sup>c</sup> Centre for Advanced Process Technology for Urban Resource Recovery (CAPTURE), Frieda Saeystraat 1, 9052 Zwijnaarde, Belgium

\* Corresponding author: [tom.breugelmans@uantwerpen.be](mailto:tom.breugelmans@uantwerpen.be)

<sup>1</sup> These authors contributed equally.

## Abstract

CO<sub>2</sub> electrolyzers require gaseous CO<sub>2</sub> or saturated CO<sub>2</sub> solutions to achieve high energy efficiency (EE) in flow reactors. However, CO<sub>2</sub> capture and delivery to electrolyzers is in most cases responsible for the inefficiency of the technology. Recently, bicarbonate zero-gap flow electrolyzers have proven to convert CO<sub>2</sub> directly from bicarbonate solutions, thus mimicking a CO<sub>2</sub> capture media, obtaining high Faradaic efficiency (FE) and partial current density (CD) towards carbon products. However, since bicarbonate electrolyzers use bipolar membrane (BPM) as a separator, the cell voltage ( $V_{\text{Cell}}$ ) is high and the system becomes less efficient compared to analogous CO<sub>2</sub> electrolyzers. Due to the role of the bicarbonate both as a carbon donor and proton donor (in contrast with gas-fed CO<sub>2</sub> electrolyzers), optimization by using know-how from conventional gas-fed CO<sub>2</sub> electrolyzers is not valid. In this study, we have investigated how different engineering aspects, widely studied for upscaling gas-fed CO<sub>2</sub> electrolyzers, influence the performance of bicarbonate zero-gap flow electrolyzers when converting CO<sub>2</sub> to formate. The temperature, the flow rate and the concentration of electrolyte are evaluated in terms of FE, productivity,  $V_{\text{Cell}}$  and EE in a broad range of current densities (10-

400 mA cm<sup>-2</sup>). CD of 50 mA cm<sup>-2</sup>, Room temperature, high flow rate (5 mL cm<sup>-2</sup>) of electrolyte and high carbon load (KHCO<sub>3</sub> 3 M) are proposed as potentially optimal parameters to benchmark a design to achieve the highest EE (27% is obtained this way), one of the most important criteria when upscaling and evaluating Carbon Capture & Conversion technologies. On the other hand, at high CD (>300 mA cm<sup>-2</sup>), low flow rate (0.5 mL cm<sup>-2</sup>) has the highest interest for downstream processing (>40 g L<sup>-1</sup> formate is obtained this way) at the cost of a low EE (<10 %).

### Keywords

Carbon Capture and Utilization, Bicarbonate reduction, zero-gap flow electrolyzers, bipolar membranes

## 1 Introduction

The increase in the concentration of CO<sub>2</sub> present in the atmosphere, currently over 415 ppm, poses a threat to society since it is directly linked to global warming and climate change.<sup>1</sup> The CO<sub>2</sub> is mostly released from anthropogenic sources as a co-product of many processes within the chemical industry (like organic synthesis or metallurgy) or after the combustion of fuels as a means of energy obtention.<sup>2,3</sup> Some of the strategies to reduce the net emissions is to reutilize the released CO<sub>2</sub> by developing technologies in the theme of Carbon Capture and Utilization (CCU). In CCU, the CO<sub>2</sub> is directly captured from the air or from flue gasses to be used as a substrate to produce high-value or bulk chemicals with processes such as methanation or electroreduction, thus valorising the CO<sub>2</sub> at the same time to make the chemical industry more sustainable.<sup>4,5</sup> The electrocatalytic conversion of CO<sub>2</sub> (eCO<sub>2</sub>R) is proposed as one of the most promising technologies to convert CO<sub>2</sub> in an efficient and green way after it has been captured.<sup>6</sup> The eCO<sub>2</sub>R consists in converting electrochemically CO<sub>2</sub> to a variety of carbon-based products (such as formate, CO, ethylene, methane and different alcohols) by using renewable electricity as an energy source and an electrocatalyst, which will determine the product formed.<sup>7-10</sup> However, one of the main drawbacks (and thus a challenge towards developing the technology) is the high energy requirement for capturing CO<sub>2</sub>, specifically from the air.<sup>11,12</sup> Since the concentration of CO<sub>2</sub> in the air is relatively very low compared to the rest of the molecules that makes up the atmosphere (like N<sub>2</sub>, O<sub>2</sub> or H<sub>2</sub>O),

obtaining it becomes cumbersome and costly. Current technologies to capture CO<sub>2</sub> in CCU include a capturing step with an alkaline solution, a regeneration step to extract back the CO<sub>2</sub> and a compression step to store the CO<sub>2</sub> to be delivered later to the electrochemical cell.<sup>13-15</sup> The last two steps require most of the total energy for capturing and converting CO<sub>2</sub>. Then, capturing and delivering the CO<sub>2</sub> efficiently to the electrochemical cell is critical to making the process feasible and industrially interesting.

To avoid these high energy demanding steps, one of the alternatives is to use bicarbonate (HCO<sub>3</sub><sup>-</sup>) aqueous solutions, such as KHCO<sub>3</sub>, as the actual reactant for the electrochemical reduction step instead of gaseous CO<sub>2</sub> or CO<sub>2</sub> purged solutions.<sup>16</sup> By using bicarbonate as substrate, there is no necessity of compressing and releasing CO<sub>2</sub> again after the capturing step, since CO<sub>2</sub> is captured in form of bicarbonate with an alkaline solution, like KOH, and then used in the electrochemical cell. Although this alternative appears to easily solve the drawback of using CO<sub>2</sub> gas as a substrate, it is still far from applicable. Bicarbonate electrolysis has proven to be less efficient in terms of Faradaic Efficiency (FE) and partial current density (CD) towards carbon products compared to analogous gas-fed CO<sub>2</sub> reduction systems and little research has been done about it. Most of the studies currently done on eCO<sub>2</sub>R involve supplying pure CO<sub>2</sub> gas to the electrochemical cell or gas diffusion electrodes instead of using post-capture CO<sub>2</sub> solutions,<sup>17</sup> mostly due to the little knowledge that the community possessed on the role of bicarbonate as a substrate (or intermediate) in eCO<sub>2</sub>R.

The role of bicarbonate in the eCO<sub>2</sub>R and the mechanism behind the electrochemical reduction of bicarbonate have been debated within the community for a long time. It is said that bicarbonate is the substrate of the reduction reaction and thus the low FE comes from the lack of the right catalyst or the unoptimized electrochemical reactor,<sup>18,19</sup> while on the other hand there is also the statement supporting that bicarbonate is merely a carbon donor, CO<sub>2</sub> being the substrate of the reaction (delivered from the equilibrium reaction of bicarbonate with water) and that the low FE comes from the high proton donor ability of bicarbonate, thus promoting the hydrogen evolution reaction (HER), the main co-reaction.<sup>20</sup> Based on the research done on this topic in the last few years, it can be concluded that in fact 1) bicarbonate is a carbon donor and supplies CO<sub>2</sub> to the surface of the electrode, even in saturated CO<sub>2</sub> solutions where there is free dissolved CO<sub>2</sub> present;<sup>21,22</sup> 2) bicarbonate is a proton donor, promoting to a great extent the HER;<sup>20,23</sup> and 3) the substrate of the

electrochemical reduction of bicarbonate is indeed  $\text{CO}_2$  instead of bicarbonate, even in pure bicarbonate solutions.<sup>24</sup> Then, to increase the FE and CD towards carbon products when using bicarbonate as a substrate there are two main strategies to follow: either the proton donor ability of bicarbonate is inhibited or the carbon donor ability of bicarbonate is promoted.

Some studies explored how to inhibit HER in bicarbonate electroreduction systems but, although high FE was obtained (more than 70%, setting a benchmark in bicarbonate conversion to formate), the partial CD was low ( $3 \text{ mA cm}^{-2}$ ) and the strategy approached involved the addition of extra components to the electrolyte, such as surfactants, that made the system more complex and harder to upscale.<sup>24,25</sup> On the other hand, some other studies explored how to improve the carbon donor ability of bicarbonate by acidifying in situ the catholyte (and thus releasing more  $\text{CO}_2$  from bicarbonate) by using a bipolar membrane (BPM) as a separator in a zero-gap flow electrolyzer, depleting water to  $\text{H}^+$  (towards the catholyte) and  $\text{OH}^-$  (towards the anolyte) upon the polarization of the electrodes (Figure 1). The results obtained by using this strategy were promising, specifically in terms of partial CD ( $50\text{-}150 \text{ mA cm}^{-2}$ ), and good FE towards formate or CO was obtained (40-60%).<sup>26,27</sup> However, since a BPM has a three-membrane layer configuration, the ohmic drop between the two electrodes is very high. In addition, an overpotential for water dissociation is added to the system thus becoming more inefficient in terms of energy efficiency of the electrochemical cell (EE) than in analogous systems involving  $\text{CO}_2$  gas and ionomeric membranes (because of the increase in the cell voltage,  $V_{\text{Cell}}$ ).<sup>28-30</sup> Nevertheless, due to its special role in bicarbonate electrolysis, the use of BPM is benchmarked for the design of bicarbonate (zero gap) electrolyzers.

As the most promising strategy, there is interest in optimizing the performance of the bicarbonate zero-gap electrolyzer involving BPM as a separator. The first approach was to find the most optimal configuration of the electrocatalyst to achieve the highest FE and partial CD towards carbon products. Most  $\text{eCO}_2\text{R}$  flow electrolyzers involve Gas Diffusion Electrodes (GDE) to avoid flooding of the electrode while the  $\text{CO}_2$  is provided from the gas phase.<sup>17</sup> To achieve these functions, the GDEs are generally formed of carbon support, a Micro-Porous Layer (MPL) and a hydrophobic PTFI layer. Since in bicarbonate electrolyzers the  $\text{CO}_2$  is delivered from the bicarbonate electrolyte, this electrocatalyst configuration was suboptimal. Lees *et al.* investigated the effect of the different layers present in a GDE for bicarbonate

electrolysis. They proposed an optimal configuration of the electrocatalyst where the MPL and PTFI layers are removed from the GDE. The increase in the hydrophobicity of the electrode was detrimental for the diffusion of CO<sub>2</sub> from bicarbonate (partial flooding of the electrode is of interest in bicarbonate electrolyzers), thus decreasing the FE and partial CD.<sup>31</sup>

Other than investigating the configuration of the electrode, there is a lack of detailed research on other engineering aspects for bicarbonate electrolysis. Therefore, there is still room for improvement on the optimization of a bicarbonate zero-gap flow electrolyzer. For this reason, we have investigated how operational parameters such as the temperature of the reactor, the inlet flow rate of the electrolyte and the concentration of carbon load affect the performance of a bicarbonate zero-gap flow electrolyzer involving a BPM. In addition, we have complemented the study on the optimization of the electrocatalyst done by Lees *et al.*, by investigating the effect of the binder material used in the composition of the electrocatalyst ink on the performance of the system. Formate is targeted as product for the bicarbonate electrolysis experiments. It is well known that formic acid is one of the key products for the valorization of eCO<sub>2</sub>R.<sup>32</sup> However, currently, eCO<sub>2</sub>R strategies pursue formate, too.<sup>33</sup> This is due to the low pK<sub>a</sub> of formic acid (3.74) which requires an acidic catholyte (thus promoting HER) or high concentration of formic acid at the outlet catholyte, otherwise formate is produced. This is hardly possible in bicarbonate electrolysis because of the mild-alkaline media of the catholyte (pH 8-9). State-of-the-art in eCO<sub>2</sub>R already considers formate as value product for energy storage, such as in formate fuel cells.<sup>34,35</sup> On the other hand, some downstream processing pathways already includes the conversion of formate to formic acid prior the separation steps. In some cases, even formate is directly separated without the necessity of converting it to formic acid first.<sup>33</sup> Therefore, formate is an ideal product to test the operational conditions of bicarbonate electrolysis. Therefore, Sn-based electrocatalyst was selected to convert bicarbonate since it is one of the most selective materials for the production of formate from bicarbonate electrolysis.<sup>36</sup> In addition, Sn has never been tested before in bicarbonate zero-gap flow electrolyzers, adding extra value to the study (only Bi has been reported).<sup>37</sup> Nevertheless, the FE towards formate from bicarbonate electrolysis is still far from optimal (up to 60% has been reported up to day),<sup>26</sup> then we must assume an important fraction of the FE towards co-reactions such as the HER and the CO formation. Based on our previous work on CO<sub>2</sub> electrolysis (where similar catalyst

configuration and operational conditions were used)<sup>38</sup> and the reports on alkaline CO<sub>2</sub>/bicarbonate electrolysis,<sup>36</sup> the main products are formate and H<sub>2</sub>. Therefore, we find negligible for this study the fraction of CO formed from bicarbonate electrolysis, thus considering the rest of the FE towards HER. Nonetheless, in research focused on CO/syngas production or in studies on the selectivity of bicarbonate electrolysis, this small fraction of FE (specifically how it evolves with high CD) must be considered. Nevertheless, the conclusions of the results obtained in this study can be easily extrapolated to other targeted products, such as CO, since the same reactor configuration is currently used.

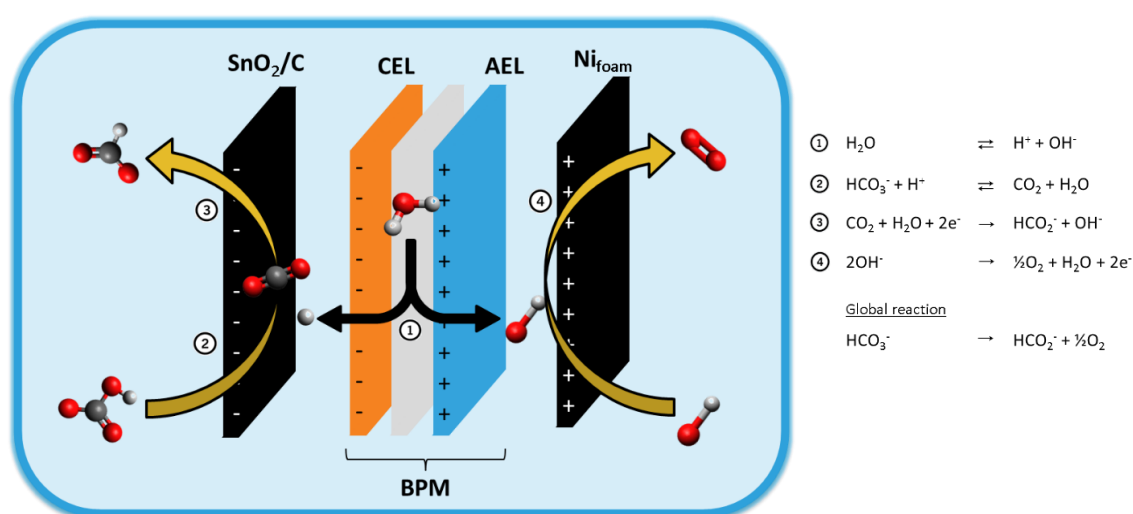


**Figure 1: Schematic representation of the mechanism of bicarbonate electrochemical reduction to formate in reactors involving a BPM (CEL: Cation Exchange Membrane. AEL: Anion Exchange Membrane).**

The FE towards formate ( $\text{FE}_{\text{Formate}}$ ), formate concentration,  $V_{\text{Cell}}$  and EE were used to evaluate and compare the performance of the electrolyzer in each case scenario for a broad range of current densities (10-400 mA cm<sup>-2</sup>). The details, assumptions and formulas used can be found in the supportive information. The FE allowed us to evaluate the selectivity of the electrolysis, the formate concentration allowed us to evaluate the profitability of the product solution for downstream processing, the  $V_{\text{Cell}}$  allowed us to evaluate the Cell efficiency (CE) of the electrolyzer and finally, the EE allowed us to evaluate the overall efficiency of the electrolysis (for upscaling prospects). For the evaluation of the effect of the binder material in the configuration of the electrode, only the FE was evaluated. At the end of this study, the most

optimal configuration(s) are proposed for benchmarking high-efficient engineering aspects for the design of a bicarbonate zero-gap flow electrolyzer.

## 2 Materials and methods

### 2.1 Materials and solutions

All the chemicals were obtained from commercial sources and used without purification unless stated otherwise.  $\text{KHCO}_3$  solutions used as catholyte were prepared by dissolving the corresponding amount of 3 M (unless stated otherwise) potassium hydrogen carbonate 99.5% (Chem-Lab) in Ultra-Pure water (MilliQ, 18.2 M $\Omega$  cm). The KOH solutions used as anolyte were prepared by dissolving the corresponding amount of 1 M of potassium hydroxide pellets (Chem-Lab) in Ultra-Pure water. Tin nanoparticles, particle size <150 nm (Sigma-Aldrich) and tin(IV) oxide nanoparticles (Sigma-Aldrich), particle size  $\leq 100$  nm were used as the catalyst and porous carbon paper AvCarb MGL 190 (Fuel Cell Store) was used as catalyst support. Nafion D-520 dispersion (Alfa Aesar) and Sustanion<sup>®</sup> XA-9 (Dioxide Materials) were used as binder ionomer during electrode manufacturing. For the counter electrode, Ni foam (Nanografi) was used. To separate the catholyte and the anolyte, a Bipolar Membrane (FumaSep) was used.

### 2.2 Working electrode manufacturing

Adding complexity to the electrocatalyst material has been questioned due to the unrealistic upscaling capabilities, even though the electrochemical response in lab-scale is proficient. For instance, complex electrodes that consists of multiple components such as nano-scaled arrangements, binders or additives present a huge variety of properties (conductivity, active sites, stability...) that, as a result, make the chemistry/structure of the surface almost impossible to correlate.<sup>39</sup> To benchmark our experimental procedure and to focus specifically on the engineering parameters of the reactor mentioned, commercial Sn (or  $\text{SnO}_2$ ) nanoparticles of particle size <150 nm are used. Del Castillo *et al.* demonstrated an optimal reduction of  $\text{CO}_2$  to formate on by using these Sn particles with a particle size of 150 nm.<sup>40</sup> We used this procedure in previous  $\text{eCO}_2\text{R}$  engineering studies and it allowed a proper evaluation of the results obtained as well as good reproducibility.<sup>41</sup> Parallely, we used  $\text{SnO}_2$  particles, too, as high performance has been observed in recent studies.<sup>42,43</sup>



Working electrodes were manufactured by spray coating a catalyst ink on top of a 4x4 cm<sup>2</sup> porous carbon paper. For the preparation of this ink, the nanoparticles (Sn or SnO<sub>2</sub>) were mixed with a 50/50 isopropanol/water solution. Optionally a binder ionomer was added to the mixture following the procedure benchmarked in our previous research (mass ratio of 70/30 nanoparticles/binder and concentration of 3 wt%).<sup>38</sup> Next a sonication probe (SinapTec NexTgen Lab 120) was used for 30 minutes to disperse the nanoparticles in the solution and create a homogenous ink. After the sonication procedure, the homogenous ink is deposited on the porous carbon substrate by airbrushing with argon as carrier gas. During the airbrushing procedure, the electrode was placed on a hotplate where the temperature was maintained at 60 °C to promote the evaporation of the solvent. Finally, the finished electrode is dried under atmospheric conditions and weighed to calculate the loading of the catalyst particles. All electrodes used in the experiments had a final loading of 2.0 ± 0.2 mg cm<sup>-2</sup> nanoparticles.

### *2.3 Electrolysis*

The electrochemical screening is performed in a custom build bicarbonate electrolyzer, of which a schematic presentation is shown in Figure 2. The electrolyte was not previously purged with an inert gas to mimic as better as possible a CO<sub>2</sub> capture solution. Then, O<sub>2</sub> reduction and CO production are assumed as artefacts of the process and as contributors to the total FE. The bicarbonate enters the electrolyzer from the bottom, where it flows through the graphite flow channel to the top of the electrolyzer. The graphite flow channel has an interdigitated design, thereby the bicarbonate is convectively forced in the pores of the working electrode which is pressed against the graphite plate. This flow design thereby optimizes the mass transfer of bicarbonate towards the catalyst surface. On top of the electrode, a BPM is placed. This BPM serves multiple purposes. 1) It separates the cathode from the anode region and thereby prevents product crossover; 2) allows the movement of ions in between the two electrodes and 3) provides the protons to the catholyte. The last purpose is essential for the good operation of the cell as the protons will dissociate the bicarbonate in water and CO<sub>2</sub>. The anode side of the electrolyzer is similar to the previously described cathode side. However, here a nickel foam was used as an electrode and potassium hydroxide as an anolyte. Copper current collectors are fitted against the backs of the graphite flow channels and are used to connect the potentiostat (Autolab PGSTAT302N) to the system. Finally, the electrolyzer is assembled using two aluminium backplates and Viton gaskets to provide sealing.

The bicarbonate solution was fed in single-pass mode to the cathode side of the electrolyzer using a High-Performance Liquid Chromatography (HPLC) pump which allowed for accurate control of the flowrate. At the outlet of the electrolyzer, a liquid/gas separator was used to separate the different phases of the flow exiting the reactor and samples were taken for product analysis. On the anode side, a peristaltic pump was used to recirculate 1000 mL of 1 M potassium hydroxide at a flow rate of 20 mL min<sup>-1</sup>. The complete electrolyzer was placed in an oven (Binder Oven) to control the temperature of the system at multiple values (25, 40 and 60 °C).

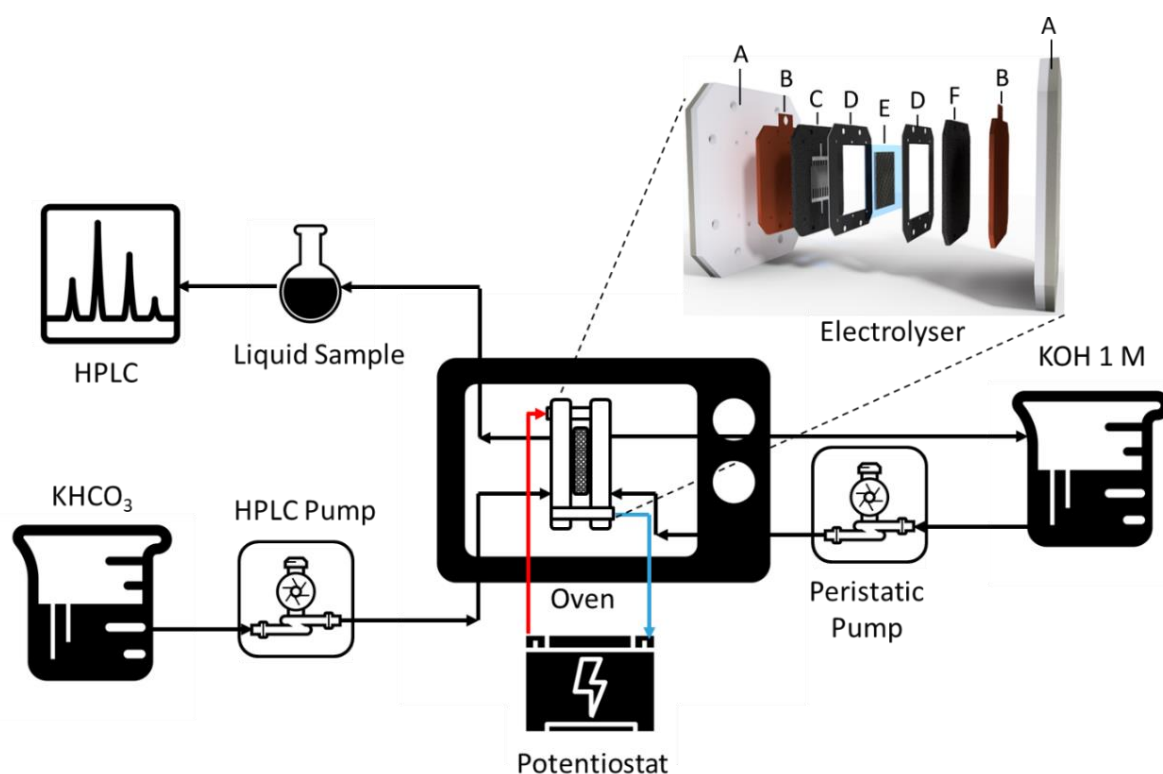


Figure 2: Schematic representation of the experimental set-up of the zero-gap electrolyzer for bicarbonate electrochemical reduction. Expanded view: A) end-plates; B) Cu current collectors; C) Cathode flow channel; D) Catalysts gaskets; E) BPM; F) Anode flow channel.

#### 2.4 Product analysis

For product analysis, Agilent 1200 High-Performance Liquid Chromatography with Agilent Hi-Plex H 7.7×300 mm column was used to separate the product and Agilent 1260 RID detector to detect and quantify formate in the form of formic acid. The samples were previously diluted with water and acidified with H<sub>2</sub>SO<sub>4</sub> to avoid bubble formation and obstruction in the column.

H<sub>2</sub>SO<sub>4</sub> 0.01 M was used as the mobile phase. Two tests per set of experiments are performed and displayed as the average of FE, the concentration of formate, Cell Voltage and EE. The error bars correspond to the standard deviation.

### 3 Results and Discussion

#### 3.1 Catalyst configuration: binder material and oxidation state

Tin-based catalysts are already well established among the preferred catalyst for the eCO<sub>2</sub>R towards formate. Recently it was shown that oxidized (IV) tin performed even better.<sup>44–46</sup> To analyse if this behaviour remains in a bicarbonate electrolyzer, we have performed experiments with porous carbon on which either Sn or SnO<sub>2</sub> nanoparticles were deposited. The results displayed in Figure 3 (left) show that at low current densities (10 mA cm<sup>-2</sup>) the FE<sub>Formate</sub> is slightly better on Sn (38%) versus SnO<sub>2</sub> (33%). However, by increasing the CD a drop in FE<sub>Formate</sub> on Sn was observed, while on SnO<sub>2</sub> drastically increased. At 25 mA cm<sup>-2</sup>, the FE<sub>Formate</sub> on SnO<sub>2</sub> nanoparticles reached a peak at 51% after which it linearly decreased to 31% at 100 mA cm<sup>-2</sup>. On Sn nanoparticles, the FE<sub>Formate</sub> drops 29% at 25 mA cm<sup>-2</sup>. Further increase of the current had little effect as the FE<sub>Formate</sub> stabilized at 30%. From these results, it is clear that in analogy to eCO<sub>2</sub>R electrolyzers, SnO<sub>2</sub> outperforms Sn.

Since in bicarbonate electrolyzers there is high competition with HER, we also evaluated the effect of the binder material used in the manufacturing of the working electrodes. The binder may have an impact on the performance of the reactor, caused by the high proton activity at the catalyst surface due to the high rate of protons generated at the BPM surface, in combination with the binder effect. A proton exchange binder such as Nafion promotes the transfer of H<sup>+</sup> to the catalytic surface, promoting HER, while an anion exchange binder like Sustainion promotes the transfer of bicarbonate ions (also a good proton donor) promoting HER as well. Overall, these phenomena promote HER and thereby lower the FE and partial CD towards formate. However, there are studies showing up the good performance of Sustainion membranes in diffusing CO<sub>2</sub> and decrease HER.<sup>47</sup> Nevertheless, these studies are focused on gas-fed electrolyzers and do not include high concentrated bicarbonate solutions as catholyte, therefore the influence of the diffusion of bicarbonate anion is hardly comparable to our system. Nevertheless, it is interesting to observe if the good CO<sub>2</sub>-diffusion properties of Sustainion overcomes the diffusion of bicarbonate anion to the surface of the electrode and thus HER. The data shown in Figure 3 (right) further confirms that the performance of the

bicarbonate electrolyzer was altered when different binder materials were used during the production process of the catalyst layer. Here the data is presented for porous carbon-coated with SnO<sub>2</sub> catalyst and either Nafion, Sustainion or no binder present. Both the Nafion and Sustainion® binders show similar behaviour, the decrease of FE<sub>Formate</sub>. At low CD the FE<sub>Formate</sub> is low. Then increasing the CD leads to a peak FE<sub>Formate</sub> at 25 mA cm<sup>-2</sup> (27% and 51% for Sustainion and Nafion respectively) and a further increase of CD results in the stabilization of FE<sub>Formate</sub>. Nevertheless, Nafion outperforms Sustainion since the concentration of bicarbonate anions is substantially higher than protons. It is shown how the diffusion of bicarbonate anion outperforms the diffusion of CO<sub>2</sub> with Sustainion, resulting in a decrease of FE<sub>Formate</sub> compared to Nafion and no-binder instead to an increase. Again, the performance of the electrolyzer in terms of FE<sub>Formate</sub> was severely limited due to the favouring of HER. When no binder was used, the FE<sub>Formate</sub> remained constant around 50%, increasing slightly to 54% at 50 mA cm<sup>-2</sup>, in contrast to the experiments with a binder, where a decrease in performance when the CD increased occurred.

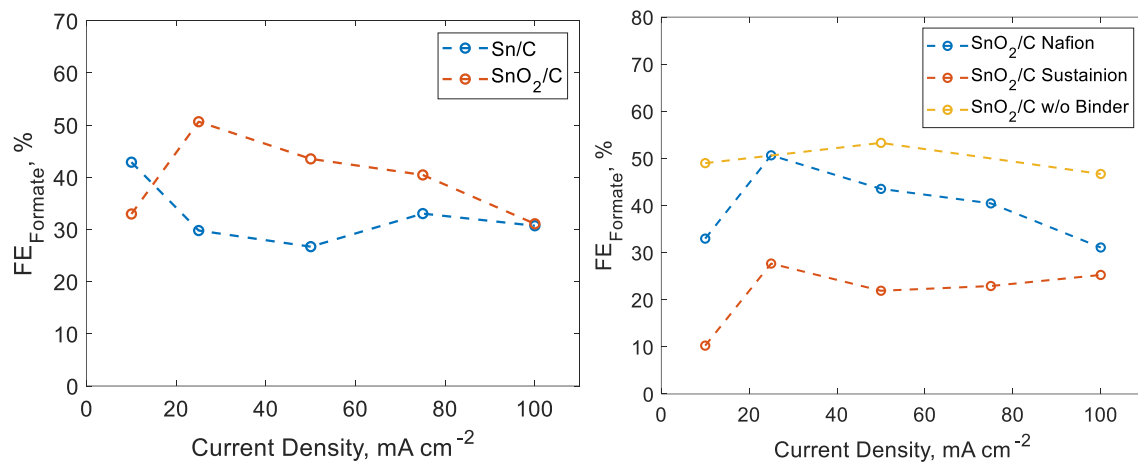


**Figure 3: FE<sub>Formate</sub> when using Sn or SnO<sub>2</sub> nanoparticles as electrocatalysts on top of a porous carbon substrate (left). FE<sub>Formate</sub> when using a SnO<sub>2</sub>/C catalyst with a Nafion binder, a Sustainion binder or without a binder (right). All the experiments were performed using a KHCO<sub>3</sub> 3 M solution at 5 mL min<sup>-1</sup> and 25 °C.**

Based on these experimental results and due to this study is not focused on the stability of the electrocatalyst, we decided to avoid using a binder as part of the ink for electrode manufacturing. We understand that, by not incorporating the binder, the stability of the electrode is compromised (as will be discussed further). However, obtaining higher FE (and

thus higher absolute values) facilitated the evaluation and comparison of the different experimental results obtained in this study. It is worth mentioning that the results obtained in this section adds further knowledge in the field of developing electrocatalyst for bicarbonate reduction, and complements the studies done so far, as mentioned previously. Therefore, SnO<sub>2</sub> coated electrodes without binder were used during the experiment as it was shown that this is the optimal composition for the conversion of bicarbonate to formate.

### *3.2 Effect of the inlet flow rate*

While research has shown that catalyst material and electrode composition are crucial in the optimization of reactor performance, it is also important to investigate the influence of process parameters, which is currently lacking in the literature. In the first set of experiments the bicarbonate flowrate is varied between 0.5 mL min<sup>-1</sup>, 1 mL min<sup>-1</sup> and 5 mL min<sup>-1</sup> while the CD is increased from 10 mA cm<sup>-2</sup> to 400 mA cm<sup>-2</sup>. The performance of the reactor (in terms of FE) is plotted versus the applied current density in Figure 4a for the different flow rates. The overall behaviour of the evolution of FE represented with the different flow rates is very similar. At low current densities, when overpotential is low, the FE towards formate (FE<sub>Formate</sub>) is between 41 and 18 % depending on the flow rate. These results are very similar to literature, where this behaviour is ascribed to the more preferred CO formation (one of the co-products often found when using Sn catalyst) at low overpotentials leading to a decrease of FE towards other carbon products such as formate, which is what we propose as an explanation of this observation.<sup>48,49</sup> However, gas phase analysis, which was not performed in this study, is needed to confirm this effect and give an exact value of FE towards CO and H<sub>2</sub>, as well as the possible energy losses present during the electrolysis. When the CD is increased towards 50 and 100 mA cm<sup>-2</sup> a sharp increase in FE<sub>Formate</sub> can be noted. A maximum FE<sub>Formate</sub> of 58 % was achieved at 5 mL min<sup>-1</sup> and 100 mA cm<sup>-2</sup>. A further increase of the CD led to a linear decrease of the FE<sub>Formate</sub>, again this is similar to literature where the co-reaction HER starts dominating at increased overpotentials.<sup>23</sup> When evaluating the effect of the flow rate in eCO<sub>2</sub>R, one of the most interesting parameters to study is the concentration of formate at the outlet of the catholyte. A lower flow rate increases the retention time of the catholyte in the electrolyzer so the final concentration of formate at the outlet flow will be higher. The cost of the downstream processing to separate the formate from the rest of the solution and valorise it depends directly on its concentration.

A higher concentration of formate decreases the operational costs of the downstream process. Former studies on the processing of products for conventional gas-fed CO<sub>2</sub> electrolyzers stated that, to be technologically feasible, the concentration of formate must be at least 45 g L<sup>-1</sup>.<sup>50</sup> Although this concentration is calculated based on the processing of gas-fed CO<sub>2</sub> electrolyzers, it can serve as a reference for bicarbonate electrolyzers, too. In figure 4b, the concentration of formate at the outlet catholyte for each case scenario is displayed. As observed, the concentration increases significantly when the flow rate decreases, as expected. For instance, at 100 mA cm<sup>-2</sup>, it increased from 2.1 to 10 and 27 g L<sup>-1</sup> when the flow rate was 5, 1 and 0.5 mL min<sup>-1</sup>, respectively. The increase in the concentration of formate is directly proportional to the flow rate although there are small variations due to the differences in the FE for each flow rate. This trend was not strictly followed along with the screening of CD when the flow rate is 0.5 mL min<sup>-1</sup> because the decrease in the FE as the CD increases is more significant (very little changes in concentration of formate from 200 to 400 mA cm<sup>-2</sup>). Interestingly when the flow rate was 0.5 mL min<sup>-1</sup>, at 200, 300 and 400 mA cm<sup>-2</sup> the concentration of formate was 40, 44 and 46 g L<sup>-1</sup> respectively, very close to the target concentration for downstream processing needed for upscaling the technology, mentioned before.

Initially, the flow rate had no noticeable influence on the V<sub>Cell</sub> since it has the same value of 2.7 V at 10 mA cm<sup>-2</sup>. Interestingly the V<sub>Cell</sub> at 5 mL min<sup>-1</sup> rose more rapidly with the CD than the experiment at 0.5 and 1 mL min<sup>-1</sup>. At 400 mA cm<sup>-2</sup>, a difference in V<sub>Cell</sub> of 800 mV was noted (figure 4c). Although with the experiments performed in this study we cannot give a precise explanation on this effect, we strongly believe the increase in the V<sub>Cell</sub> at high CD and high flow rate is caused by the loss of the stability of the electrode/electrolyte interface. More detailed research involving techniques such as Electrochemical Impedance Spectroscopy would give further information and a proper evaluation of this effect. Therefore, for the flow rates studied, since the changes in the V<sub>Cell</sub> were not significant, the variation in the EE is mostly given by the FE, following the same trend. Then, as the CD increases, the effect of the increase of the V<sub>Cell</sub> becomes noticeable and the EE decreased. The most energy-efficient systems were found at 5 mL min<sup>-1</sup> and 10 and 50 mA cm<sup>-2</sup> (27 %).

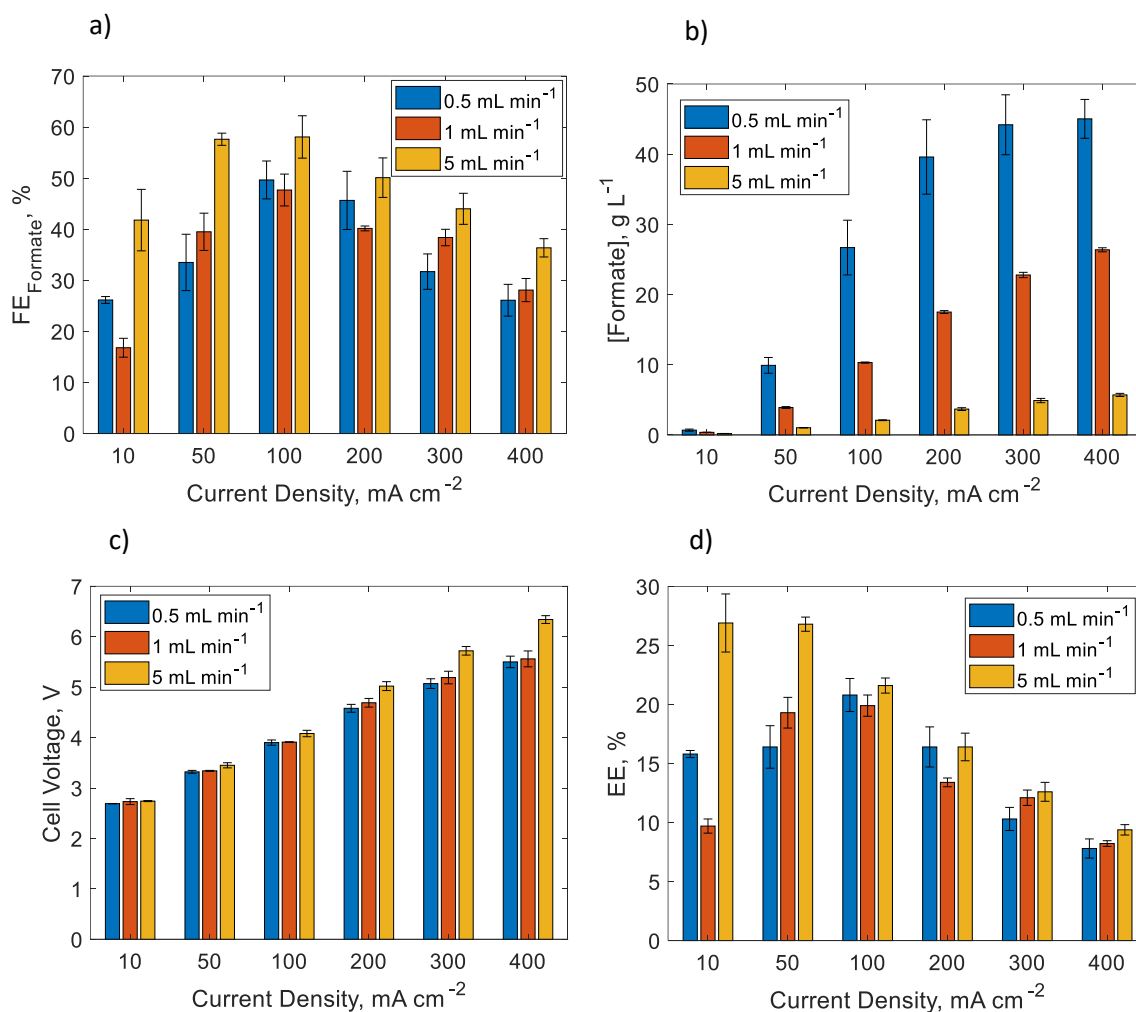


Figure 4: FE<sub>Formate</sub> (a), concentration of formate (b), V<sub>cell</sub> (c) and EE (d) of the electrolysis of a KHCO<sub>3</sub> 3 M solution with a flow rate of catholyte of 0.5, 1 or 5 mL min<sup>-1</sup>. All the experiments were performed using a SnO<sub>2</sub>/C electrocatalyst and KHCO<sub>3</sub> 3 M at 25 °C.

From the results described above, it is clear that the most efficient performance was obtained at increased bicarbonate flowrate, although the difference is only noticeable at 5 mL min<sup>-1</sup>. Little difference was found between 0.5 and 1 mL min<sup>-1</sup>. It is hypothesized that this is caused due to the longer residence time of the in-situ generated gas bubbles at a lower flow rate such as 0.5 and 1 mL min<sup>-1</sup> (mainly CO<sub>2</sub> and H<sub>2</sub>). These bubbles will cover part of the catalyst surface and thereby will reduce the overall electrochemical active surface area, which obviously will negatively affect the cell's performance. However, by increasing the flow rate of the bicarbonate, the gas/liquid ratio of the cell will decrease (e.g. more liquid will be present in the cell) and thus less of the catalyst surface will be shielded, resulting in higher FE<sub>Formate</sub> and EE. In addition to CO<sub>2</sub>, most of the gas formed is H<sub>2</sub> produced during the reaction. When the flow

rate is low, these H<sub>2</sub> bubbles stay on the surface of the electrode or in the zero-gap interface, decreasing the performance of the reactor. A higher electrolyte flow rate will mechanically remove the H<sub>2</sub> bubbles and allow most of the surface of the electrode to be fully operational for the duration of the experiment. Additionally, an increased flow rate will increase the turbulence in the cell and thereby promote the convective mass transfer of (ionic) species towards and away from the electrochemically active surface and mass transport-related losses are reduced. Finally, the retention time of the produced formate in the cell is lower at an increased flow rate, thus the crossover flux through the membrane is smaller. However, as shown in literature the crossover through BPM is rather limited thus this effect will be minimal.<sup>51,52</sup>

### *3.3 Effect of the temperature of the electrolyzer*

We studied the effect of the temperature by building the electrolyzer up in an oven and fixing the value of the temperature in a way that the whole reactor is in isothermal conditions. By doing this, not only the KHCO<sub>3</sub> electrolyte but also the electrodes and the rest of the components of the electrolyzer will be affected by the temperature. We expected to affect the system in different ways by changing the temperature. First, the electrochemical thermodynamic parameters, such as the electrochemical reduction and oxidation potentials ( $E_{\text{red}}$  in the cathode and  $E_{\text{ox}}$  in the anode), will be decreased with the increase of temperature, as the Nernst equation indicates, leading to a decrease in the  $V_{\text{cell}}$ . On the other hand, the solubility of CO<sub>2</sub> (already low at room temperature, 0.033 M) will decrease with the increase of temperature, as Henry's law indicates and we show in Figure S1. For instance, at 40 °C the solubility of CO<sub>2</sub> in water is 0.026 M and at 60 °C the solubility is 0.018 M, decreasing the amount of dissolved CO<sub>2</sub> in the electrolyte. In a bicarbonate solution, there is always a fraction of dissolved CO<sub>2</sub> derived from the equilibrium of bicarbonate with water, which is determined by the pH (see Bjerrum plot, Figure S2). At the working pH of 8.3, this fraction is 1.2%. Therefore, in a 3 M KHCO<sub>3</sub> solution, there is 0.036 M of dissolved CO<sub>2</sub> which is higher than the solubility of CO<sub>2</sub> in water at 25 °C, 0.033 M. Thus, in a 3 M KHCO<sub>3</sub> solution at 25 °C only 0.033 M remains as dissolved CO<sub>2</sub>. As the temperature increases, not only does the solubility of CO<sub>2</sub> decrease but the solubility of KHCO<sub>3</sub> increases<sup>53</sup> stabilizing the solution to detriment of the depletion of HCO<sub>3</sub><sup>-</sup> to dissolved CO<sub>2</sub> and H<sub>2</sub>O. Since in bicarbonate electrolysis the dissolved CO<sub>2</sub> is the active substrate of the reaction instead of CO<sub>2</sub> gas, it means a decrease in the amount



of available  $\text{CO}_2$  to react and thus a decrease in the FE. In addition, the thermodynamic acidic constant ( $K_{a1}$ ) of the equilibrium reaction between  $\text{HCO}_3^-$  and  $\text{CO}_2$  will be modified. The increase in temperature increases the value of the  $K_{a1}$ , meaning that the ratio  $\text{HCO}_3^-/\text{CO}_2$  will increase in favour of  $\text{HCO}_3^-$  (more  $\text{HCO}_3^-$  and less  $\text{CO}_2$  will be present at equilibrium after the BPM donates  $\text{H}^+$ ). Furthermore, the ionic conductivity of the electrolyte will increase favouring the mobility of ions, thus decreasing the resistivity of the electrolyte and improving the  $V_{\text{Cell}}$ . However, combined with the higher permeability acquired by the membrane, it might lead to product crossover, although the corresponding analysis is out of the scope of this study. We must take account the effect of the temperature on the competing reaction, HER, too. Protons are less likely to be affected by mass transport compared to  $\text{HCO}_3^-$  or  $\text{CO}_2$ , thus an increase in temperature should favor HER. Then, we can assume that increasing the temperature is favourable for decreasing the  $V_{\text{Cell}}$  but unfavourable for the electrochemical conversion of  $\text{CO}_2$  (FE) since less dissolved  $\text{CO}_2$  and more  $\text{HCO}_3^-$  and  $\text{H}^+$  (HER promoters) will be available in the reactor. However, we also must take into account the effect of the temperature in the kinetics of the reaction and the diffusion of reactants. The increase of temperature promotes the exchange current density and the diffusion constant and thus the reaction rate of  $\text{CO}_2$  to formate. Nevertheless, we must investigate if the increase in the kinetics of the reaction and the decrease of the  $V_{\text{Cell}}$  is enough to overcome the drawbacks of decreasing the solubility of  $\text{CO}_2$  and increasing the rate of  $\text{HCO}_3^-/\text{CO}_2$  in the electrolyte. In this regard, the EE is a parameter that can be used to evaluate the performance of each system since we can then compare both the contributions of the temperature to the  $V_{\text{Cell}}$  and the conversion of  $\text{CO}_2$  (FE).

To properly evaluate the effect of temperature we performed electrolysis at 25, 40 and 60 °C fixing the concentration of  $\text{KHCO}_3$  at 3 M and the flow rate at 5 mL  $\text{min}^{-1}$ . As shown in Figure 5a, the  $\text{FE}_{\text{Formate}}$  decreases with the increase of temperature at CD below 100  $\text{mA cm}^{-2}$  (for instance 58, 51 and 43% at 25, 40 and 60 °C respectively) confirming the mentioned effect of the lack of dissolved  $\text{CO}_2$  present, the increase in the solubility of  $\text{KHCO}_3$  and the HER promotion at increased temperatures. After 100  $\text{mA cm}^{-2}$ , the difference of the  $\text{FE}_{\text{Formate}}$  at 25 and 40 °C is not significant (44% at 300  $\text{mA cm}^{-2}$ ), but it still decreases at 60 °C (41% at 300  $\text{mA cm}^{-2}$ ). At 40 °C the decrease in the concentration of dissolved  $\text{CO}_2$  is compensated by the improvement in the kinetics of the reaction and the diffusion when the CD is over 100  $\text{mA cm}^{-2}$ . Below 100  $\text{mA cm}^{-2}$ , these improvements are not compensating for the lack of dissolved  $\text{CO}_2$

present in the electrolyte. At CD higher than  $100 \text{ mA cm}^{-2}$ , the  $FE_{\text{Formate}}$  is similar to  $25 \text{ }^\circ\text{C}$ , in contrast with  $60 \text{ }^\circ\text{C}$ , where even at high CD the low solubility of  $\text{CO}_2$  is more significant than the increase in kinetics. Another observation is that the highest  $FE_{\text{Formate}}$  obtained at  $25 \text{ }^\circ\text{C}$  is at  $50 \text{ mA cm}^{-2}$  (58%), while at  $40$  and  $60 \text{ }^\circ\text{C}$  it is at  $100 \text{ mA cm}^{-2}$  (59 and 52% respectively), confirming the improvement in the kinetics of the reaction when the temperature is increased (the reaction is kinetically controlled at larger voltage). Interestingly, there is a slight shift in the trend of  $FE_{\text{Formate}}$  at increased temperature when the CD is  $>200 \text{ mA cm}^{-2}$ . This can be caused by the change in the selectivity of the reaction. As mentioned before, at higher CD, CO formation and HER are promoted, leading to a decrease in  $FE_{\text{Formate}}$ . This is an interesting effect worth of study for following bicarbonate electrolysis evaluation. In this case and contrast with the flow rate, the difference of the concentration of formate at the outlet catholyte with the temperature appears to be solely dependent on the FE, as it follows the same trend (higher FE, higher concentration). Since formic acid is not a very volatile compound at mild conditions (boiling point  $101 \text{ }^\circ\text{C}$  at 1 atm) there is not any special effect of applying  $40$  and  $60 \text{ }^\circ\text{C}$  (Figure 5b).

If we take a look at the EE (Figure 5d), although the  $FE_{\text{Formate}}$  is lower, the system is more efficient at converting  $\text{CO}_2$  to formate at  $40$  and  $60 \text{ }^\circ\text{C}$  when the CD is higher than  $100 \text{ mA cm}^{-2}$  (13 and 14% EE at  $300 \text{ mA cm}^{-2}$  at  $40$  and  $60 \text{ }^\circ\text{C}$  respectively), due to the drastic decrease of the  $V_{\text{cell}}$  induced to the system (from  $5.7$  at  $25 \text{ }^\circ\text{C}$  to  $5.4$  and  $4.8 \text{ V}$  at  $300 \text{ mA cm}^{-2}$  at  $40$  and  $60 \text{ }^\circ\text{C}$  respectively) and the decrease of the electrolyte resistivity (Figure 5c). However, the most energy-efficient system was still at  $25 \text{ }^\circ\text{C}$ , specifically when  $50 \text{ mA cm}^{-2}$  were applied (27 %). We can then conclude that the effect of increasing the temperature is beneficial when working at a higher CD than  $100 \text{ mA cm}^{-2}$ , where the decrease in the  $V_{\text{cell}}$  has a huge impact on the EE of the system. However, CD below  $100 \text{ mA cm}^{-2}$  is still desired for achieving the highest EE. In addition, taking into account that for the EE calculations we did not consider the energy invested to heat up the system to the desired temperature (since it is a very variable parameter that depends on the setup used) we can further conclude that there is no interest in increasing the temperature if we want to achieve higher EE. This adds value to the technology as the best performance is at room temperature, a very attractive parameter for upscaling the technology.

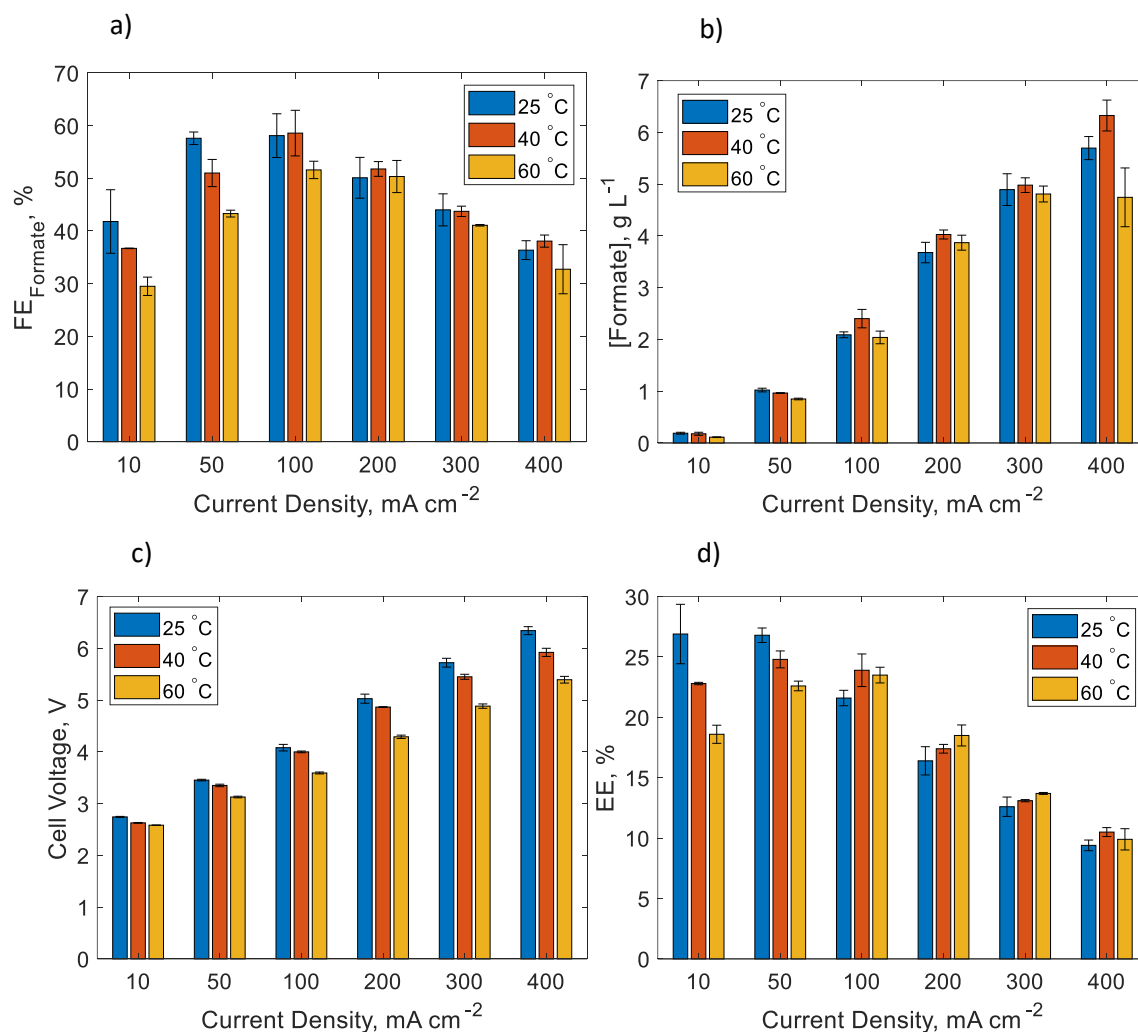


Figure 5: FE<sub>Formate</sub> (a), concentration of formate (b), V<sub>Cell</sub> (c) and EE (d) of the electrolysis of a KHCO<sub>3</sub> solution at 25, 40 and 60 °C. All the experiments were performed using a SnO<sub>2</sub>/C electrocatalyst and KHCO<sub>3</sub> 3 M at 5 mL min<sup>-1</sup>.

### 3.4 Effects of the concentration of carbon load (bicarbonate)

To increase the FE towards CO<sub>2</sub>R products from KHCO<sub>3</sub> electrolytes it is desired to use as high concentration of KHCO<sub>3</sub> as possible since then the highest amount of dissolved CO<sub>2</sub> will be present (for instance 0.036 M CO<sub>2</sub> in KHCO<sub>3</sub> 3 M, comparable to saturated CO<sub>2</sub> solutions, 0.033 M).<sup>24</sup> However, obtaining a 3 M KHCO<sub>3</sub> solution from direct air capture (DAC) or flue gas capture using KOH solution as capturing agent is still unrealistic and ambitious from an industrial point of view due to the low amount of CO<sub>2</sub> present in the air (415 ppm) and thus the low concentrated KHCO<sub>3</sub> solution obtained during the capturing step. For the experiments performed in this study up to this section, the concentration of the solution of KHCO<sub>3</sub> used as

electrolyte was 3 M since the highest concentration of CO<sub>2</sub> dissolved can be achieved and it was the state-of-the-art solution used in previous reports.<sup>26,31</sup> However, KHCO<sub>3</sub> 3 M is an oversaturated solution, thus unstable over time and unrealistic from a CO<sub>2</sub> capture technology perspective. For this reason, we electrolyzed unsaturated KHCO<sub>3</sub> solutions and compared them to the oversaturated KHCO<sub>3</sub> 3 M solution to evaluate if the zero-gap electrolyzer can still convert CO<sub>2</sub> from less concentrated KHCO<sub>3</sub> solutions. To perform these experiments, we fixed the temperature to 25 °C and the flow rate to 5 mL min<sup>-1</sup> and we used KHCO<sub>3</sub> solutions of 1, 2 and 3 M as electrolytes. It is important to mention that, even though the initial concentration of KHCO<sub>3</sub> used as catholyte is 1, 2 or 3 M, once inside the zero-gap electrolyzer the composition of the catholyte in the electrode-membrane interface varies mainly due to the polarization of the electrode and the water depletion occurring at the BPM.<sup>28,30</sup> The main scientific reasoning says that higher concentration of bicarbonate increases the buffer strength of the catholyte, and the protons delivered from the BPM are neutralized more efficiently, releasing more CO<sub>2</sub> and decreasing HER. Nevertheless, a combination of dynamic modelling of the processes undergoing in the electrode-membrane interface with experimental data of the analysis of the inlet/outlet catholyte is needed to deliver a proper approach on the concentration of each specie in the electrolyzer. However, in this section we can compare the productivity and energetic parameters of different inlet KHCO<sub>3</sub> solutions by fixing the rest of operational conditions (membrane, catalyst, flow rate and temperature).

The results in Figure 6a show how the FE<sub>Formate</sub> decreases when the concentration of KHCO<sub>3</sub> decreases, which was expected since less dissolved CO<sub>2</sub> and carbon donor (KHCO<sub>3</sub>) is present in the electrolyte (0.036, 0.024 and 0.012 M CO<sub>2</sub> in KHCO<sub>3</sub> 3, 2 and 1 M respectively). For instance, at 100 mA cm<sup>-2</sup>, the FE<sub>Formate</sub> goes from 58 to 41 and 33% when the concentration of KHCO<sub>3</sub> is 3, 2 and 1 M, respectively. The trend of FE<sub>Formate</sub> with the CD is the same for every KHCO<sub>3</sub> concentration used: there is an increase in the FE<sub>Formate</sub> up to 50 mA cm<sup>-2</sup> and then it decreases (slowly in KHCO<sub>3</sub> 3 M electrolytes) as the CD increases, forming a plateau from 300 mA cm<sup>-2</sup> onwards when the concentration of KHCO<sub>3</sub> is 2 and 1 M. As shown, the FE<sub>Formate</sub> when using unsaturated KHCO<sub>3</sub> solutions is relatively high taking into consideration the low concentration of dissolved CO<sub>2</sub> present, although the highest FE<sub>Formate</sub> obtained is still when using oversaturated KHCO<sub>3</sub> solutions as electrolyte (as thus higher dissolved CO<sub>2</sub> present). For instance, 41% of FE<sub>Formate</sub> at 50 mA cm<sup>-2</sup> when using KHCO<sub>3</sub> 1 M as an electrolyte is an

interesting result for upscaling technologies, taking into account that the amount of dissolved  $\text{CO}_2$  in a  $\text{KHCO}_3$  1 M solution is 0.012 M (three times less than a saturated  $\text{CO}_2$  and  $\text{KHCO}_3$  solution). This is likely caused by the proton donor ability of bicarbonate, less dominating when the concentration is lower like 1 M. The changes in the concentration of formate at the outlet catholyte with the different concentration of bicarbonate follow the same trend as the FE like it happened in the case of the temperature (Figure 6b). Therefore, there is not a special role of the initial concentration of  $\text{KHCO}_3$  on the final concentration of formate, as expected.

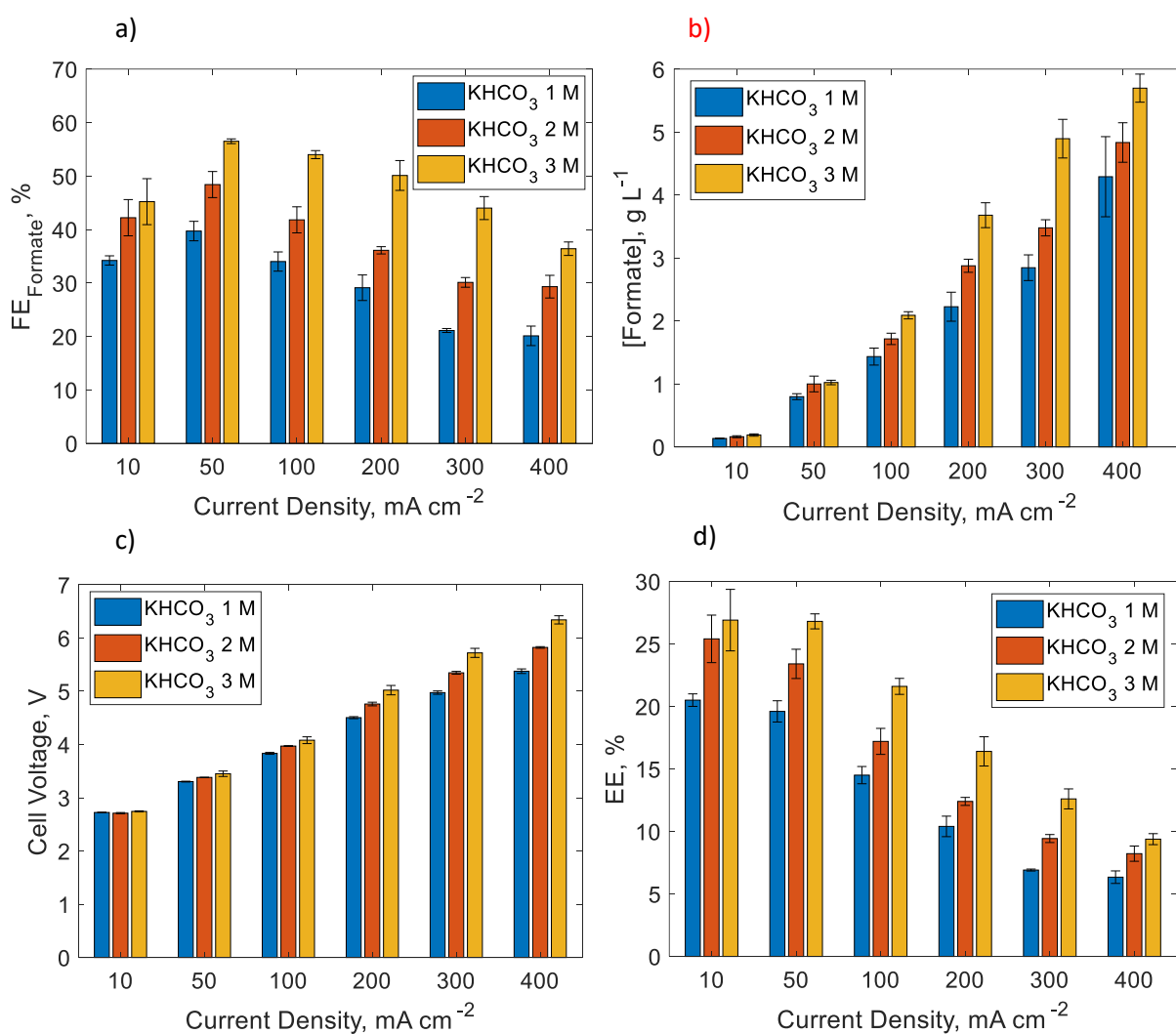


Figure 6:  $\text{FE}_{\text{Formate}}$  (a), concentration of formate (b),  $V_{\text{Cell}}$  (c) and EE (d) of the electrolysis of  $\text{KHCO}_3$  solutions of 1, 2 and 3 M. All the experiments were performed using a  $\text{SnO}_2/\text{C}$  electrocatalyst and at  $5 \text{ mL min}^{-1}$  and  $25 \text{ }^\circ\text{C}$ .

The  $V_{\text{Cell}}$  also decreased when the concentration of  $\text{KHCO}_3$  decreased (Figure 6c). This effect is better observed at high CD, as we previously explained when discussing the effects of the

flowrate (vide supra). However, in this case, there is another parameter to consider. As observed, the  $V_{\text{Cell}}$  is not directly linked to the  $FE_{\text{Formate}}$  like it did when the flow rate was studied. For instance, from  $50 \text{ mA cm}^{-2}$  onwards, the difference in the  $FE_{\text{Formate}}$  between the three concentrations of  $\text{KHCO}_3$  used remained similar (approximately 15% between 3 and 2 M and 8% between 2 and 1 M) but the difference in the  $V_{\text{Cell}}$  increases with the CD. This is because  $\text{KHCO}_3$  loses buffering effect as the concentration decreases, meaning that the acidification of the catholyte by the depletion of  $\text{H}_2\text{O}$  in the BPM will decrease the local pH close to the surface of the electrode and thus increase the concentration of  $\text{H}^+$ , decreasing the overall  $V_{\text{Cell}}$ . Even though the  $V_{\text{Cell}}$  decreases when the concentration of  $\text{KHCO}_3$  decreases (for instance 4.9, 5.3 and 5.9 V at  $300 \text{ mA cm}^{-2}$  for  $\text{KHCO}_3$  1, 2 and 3 M respectively) and then we should expect an increase in the EE of the process, the EE of the conversion of  $\text{CO}_2$  is still higher as the concentration of  $\text{KHCO}_3$  is higher (Figure 6d). For instance, 15, 17 and 22% at  $100 \text{ mA cm}^{-2}$  for  $\text{KHCO}_3$  1, 2 and 3 M, respectively. Therefore, in this case, the increase in the  $FE_{\text{Formate}}$  has a higher impact on the overall EE than the increase in  $V_{\text{Cell}}$ . The most energy-efficient experiment, 27 %, was when using  $\text{KHCO}_3$  3 M at  $50 \text{ mA cm}^{-2}$  since the  $FE_{\text{Formate}}$  obtained is the highest (58%) and the polarization of the electrode is not enough to increase the  $V_{\text{Cell}}$  significantly (3.3, 3.4 and 3.5 V for  $\text{KHCO}_3$  1, 2 and 3 M respectively).

#### 4 Conclusions

Due to the necessity to reduce the costs of the overall  $\text{CO}_2$  Capture and Conversion systems, the attention is focused not only on the optimization of the  $\text{CO}_2$  electrochemical reactors but also on the capture and release of  $\text{CO}_2$  to the electrochemical cell. Bicarbonate reduction, which was declared inefficient and its applicability was in doubt, is starting to gain attention since it is one of the most promising routes towards developing an efficient integrated  $\text{CO}_2$  capture and conversion system involving the electrochemical reduction of  $\text{CO}_2$ . Thanks to the recent knowledge gained in reactor design and on the mechanism of bicarbonate reduction, the process is now feasible at a lab scale and easier to be upscaled. In this manuscript, we have displayed how different engineering aspects such as the inlet flow rate, the temperature of the reactor or the concentration of bicarbonate, not yet evaluated for the current reactor used for bicarbonate conversion (zero-gap electrolyzer involving a BPM as a separator) affect the parameters often used to evaluate the performance of an  $\text{eCO}_2\text{R}$  electrolyzer such as the CD, the FE, the concentration of product formed, the  $V_{\text{Cell}}$  and the EE. Overall, the most efficient

systems were found at low CD (10, 50 mA cm<sup>-2</sup>), high flow rate (5 mL min<sup>-1</sup>), room temperature and high KHCO<sub>3</sub> concentration (3 M), with a maximum EE of 27% (well comparable to commonly reported EE in gas-fed CO<sub>2</sub> electrolyzers). Nevertheless, from a product processing perspective, the most interesting system is found at a low flow rate (> 40 g L<sup>-1</sup> of formate were produced at 0.5 mL min<sup>-1</sup>). However, there is still room to improve the performance of the bicarbonate electrolyzer. It is observed that the best performance was obtained at 5 mL min<sup>-1</sup>, then it is interesting to evaluate in further research the effect of higher flow rate, for instance at 50 mL min<sup>-1</sup>. On the other hand, one of the biggest reasons for the loss of EE of the system is the increase of V<sub>cell</sub> with the applied CD due to the use of BPM. Therefore, new and more optimized BPM can be used to minimize the Ohmic drop which requires to be alert on the research done on BPM technology, since it is a relatively new field of application for eCO<sub>2</sub>R (few commercial BPM are currently available). Additionally, the decrease of Ohmic drop would enable testing higher CDs (> 400 mA cm<sup>-2</sup>) at lower V<sub>cell</sub>. Other options for membranes have been considered, however, the ability of BPM to maintain the pH gradients and product crossover (in addition to the additional application of generating protons to produce CO<sub>2</sub> from bicarbonate) makes the BPM the best choice for upscaling bicarbonate electrolyzers.<sup>54</sup> Further understanding of the effects of different parameters, such as the ones considered in our study, on the ohmic and the charge transfer resistance of the reactor is still needed. For example, elaborating a deep study including techniques such as Electrochemical Impedance Spectroscopy will allow us to understand better how the flow rate and the retention of bubbles affect the performance of the bicarbonate zero-gap electrolyzer. Another urgent approach we are currently following is to target other carbon products which high valorization, such as methanol or C<sub>2</sub> products, by testing Cu-based electrocatalyst, still unreported. Finally, the electrocatalyst can be further optimized, especially focusing on its stability. The system's EE drops to 27 to 17% after 3 hours of reaction time (Figure S3) which is assumed because of the loss of catalyst activity, probably caused by the lack of binder material during the electrode manufacturing (Figure S4).<sup>55,56</sup> Nonetheless the findings in this work show promising results towards the implementation of fine-designed bicarbonate electrolyzers for the integrated capture and conversion of CO<sub>2</sub>.

## Supporting Information

Formulas and equations, Bjerrum plot, Henry's law's model, stability test, etc.

## Conflicts of interest

There are no conflicts to declare.

## Acknowledgements

O.G.S. is supported by a PhD grant from VITO's strategic research funds (project no. 1810257). B.D.M is supported by the University of Antwerp's Strategic Basic Research Industrial Research Fund (BSO-IOF) (project no. FFI170350). This research was also supported by the project CAPTIN (under the Moonshot initiative of VLAIO/Catalisti, Grant number HBC.2019.0076).

## References

- (1) Aresta, M. Carbon Dioxide: Utilization Options to Reduce Its Accumulation in the Atmosphere. In *Carbon Dioxide as Chemical Feedstock*; Wiley-VCH Verlag GmbH & Co. KGaA: Weinheim, Germany; pp 1–13. <https://doi.org/10.1002/9783527629916.ch1>.
- (2) Nagelkerken, I.; Connell, S. D. Global Alteration of Ocean Ecosystem Functioning Due to Increasing Human CO<sub>2</sub> Emissions. *Proceedings of the National Academy of Sciences* **2015**, *112* (43), 13272–13277. <https://doi.org/10.1073/pnas.1510856112>.
- (3) Dietz, T.; Rosa, E. A. Effects of Population and Affluence on CO<sub>2</sub> Emissions. *Proceedings of the National Academy of Sciences* **1997**, *94* (1), 175–179. <https://doi.org/10.1073/pnas.94.1.175>.
- (4) Grim, R. G.; Huang, Z.; Guarnieri, M. T.; Ferrell, J. R.; Tao, L.; Schaidle, J. A. Transforming the Carbon Economy: Challenges and Opportunities in the Convergence of Low-Cost Electricity and Reductive CO<sub>2</sub> Utilization. *Energy & Environmental Science* **2020**, *13* (2), 472–494. <https://doi.org/10.1039/C9EE02410G>.
- (5) Sullivan, I.; Goryachev, A.; Digdaya, I. A.; Li, X.; Atwater, H. A.; Vermaas, D. A.; Xiang, C. Coupling Electrochemical CO<sub>2</sub> Conversion with CO<sub>2</sub> Capture. *Nature Catalysis* **2021**, *4* (11), 952–958. <https://doi.org/10.1038/s41929-021-00699-7>.
- (6) Sánchez, O. G.; Birdja, Y. Y.; Bulut, M.; Vaes, J.; Breugelmans, T.; Pant, D. Recent Advances in Industrial CO<sub>2</sub> Electroreduction. *Current Opinion in Green and Sustainable Chemistry* **2019**, *16*, 47–56. <https://doi.org/10.1016/j.cogsc.2019.01.005>.



- (7) Choukroun, D.; Pacquets, L.; Li, C.; Hoekx, S.; Arnouts, S.; Baert, K.; Hauffman, T.; Bals, S.; Breugelmans, T. Mapping Composition–Selectivity Relationships of Supported Sub-10 Nm Cu–Ag Nanocrystals for High-Rate CO<sub>2</sub> Electroreduction. *ACS Nano* **2021**, acsnano.1c04943. <https://doi.org/10.1021/acsnano.1c04943>.
- (8) Karapinar, D.; Creissen, C. E.; Rivera de la Cruz, J. G.; Schreiber, M. W.; Fontecave, M. Electrochemical CO<sub>2</sub> Reduction to Ethanol with Copper-Based Catalysts. *ACS Energy Letters* **2021**, *6* (2), 694–706. <https://doi.org/10.1021/acseenergylett.0c02610>.
- (9) Artz, J.; Müller, T. E.; Thenert, K.; Kleinekorte, J.; Meys, R.; Sternberg, A.; Bardow, A.; Leitner, W. Sustainable Conversion of Carbon Dioxide: An Integrated Review of Catalysis and Life Cycle Assessment. *Chemical Reviews* **2018**, *118* (2), 434–504. <https://doi.org/10.1021/acs.chemrev.7b00435>.
- (10) Zhao, S.; Li, S.; Guo, T.; Zhang, S.; Wang, J.; Wu, Y.; Chen, Y. Advances in Sn-Based Catalysts for Electrochemical CO<sub>2</sub> Reduction. *Nano-Micro Letters* **2019**, *11* (1), 62. <https://doi.org/10.1007/s40820-019-0293-x>.
- (11) Brandl, P.; Bui, M.; Hallett, J. P.; Mac Dowell, N. Beyond 90% Capture: Possible, but at What Cost? *International Journal of Greenhouse Gas Control* **2021**, *105*, 103239. <https://doi.org/10.1016/j.ijggc.2020.103239>.
- (12) Oh, S.-Y.; Binns, M.; Cho, H.; Kim, J.-K. Energy Minimization of MEA-Based CO<sub>2</sub> Capture Process. *Applied Energy* **2016**, *169*, 353–362. <https://doi.org/10.1016/j.apenergy.2016.02.046>.
- (13) Rinberg, A.; Bergman, A. M.; Schrag, D. P.; Aziz, M. J. Alkalinity Concentration Swing for Direct Air Capture of Carbon Dioxide. *ChemSusChem* **2021**, cssc.202100786. <https://doi.org/10.1002/cssc.202100786>.
- (14) Keith, D. W.; Holmes, G.; St. Angelo, D.; Heidel, K. A Process for Capturing CO<sub>2</sub> from the Atmosphere. *Joule* **2018**, *2* (8), 1573–1594. <https://doi.org/10.1016/j.joule.2018.05.006>.
- (15) Gutiérrez-Sánchez, O.; Bohlen, B.; Daems, N.; Bulut, M.; Pant, D.; Breugelmans, T. A State-of-the-Art Update on Integrated CO<sub>2</sub> Capture and Electrochemical Conversion Systems. *ChemElectroChem* **2022**. <https://doi.org/10.1002/celc.202101540>.
- (16) Welch, A. J.; Dunn, E.; DuChene, J. S.; Atwater, H. A. Bicarbonate or Carbonate Processes for Coupling Carbon Dioxide Capture and Electrochemical Conversion. *ACS Energy Letters* **2020**, *5* (3), 940–945. <https://doi.org/10.1021/acseenergylett.0c00234>.

- (17) Wakerley, D.; Lamaison, S.; Wicks, J.; Clemens, A.; Feaster, J.; Corral, D.; Jaffer, S. A.; Sarkar, A.; Fontecave, M.; Duoss, E. B.; Baker, S.; Sargent, E. H.; Jaramillo, T. F.; Hahn, C. Gas Diffusion Electrodes, Reactor Designs and Key Metrics of Low-Temperature CO<sub>2</sub> Electrolysers. *Nature Energy* **2022**, *7* (2), 130–143. <https://doi.org/10.1038/s41560-021-00973-9>.
- (18) Bonet Navarro, A.; Nogalska, A.; Garcia-Valls, R. Direct Electrochemical Reduction of Bicarbonate to Formate Using Tin Catalyst. *Electrochem* **2021**, *2* (1), 64–70. <https://doi.org/10.3390/electrochem2010006>.
- (19) Sreekanth, N.; Phani, K. L. Selective Reduction of CO<sub>2</sub> to Formate through Bicarbonate Reduction on Metal Electrodes: New Insights Gained from SG/TC Mode of SECM. *Chem. Commun.* **2014**, *50* (76), 11143–11146. <https://doi.org/10.1039/C4CC03099K>.
- (20) Goyal, A.; Marcandalli, G.; Mints, V. A.; Koper, M. T. M. Competition between CO<sub>2</sub> Reduction and Hydrogen Evolution on a Gold Electrode under Well-Defined Mass Transport Conditions. *J Am Chem Soc* **2020**, *142* (9), 4154–4161. <https://doi.org/10.1021/jacs.9b10061>.
- (21) Deng, W.; Yuan, T.; Chen, S.; Li, H.; Hu, C.; Dong, H.; Wu, B.; Wang, T.; Li, J.; Ozin, G. A.; Gong, J. Effect of Bicarbonate on CO<sub>2</sub> Electroreduction over Cathode Catalysts. *Fundamental Research* **2021**, *1* (4), 432–438. <https://doi.org/10.1016/j.fmre.2021.06.004>.
- (22) Dunwell, M.; Lu, Q.; Heyes, J. M.; Rosen, J.; Chen, J. G.; Yan, Y.; Jiao, F.; Xu, B. The Central Role of Bicarbonate in the Electrochemical Reduction of Carbon Dioxide on Gold. *J Am Chem Soc* **2017**, *139* (10), 3774–3783. <https://doi.org/10.1021/jacs.6b13287>.
- (23) Ooka, H.; Figueiredo, M. C.; Koper, M. T. M. Competition between Hydrogen Evolution and Carbon Dioxide Reduction on Copper Electrodes in Mildly Acidic Media. *Langmuir* **2017**, *33* (37), 9307–9313. <https://doi.org/10.1021/acs.langmuir.7b00696>.
- (24) Gutiérrez-Sánchez, O.; Daems, N.; Offermans, W.; Birdja, Y. Y.; Bulut, M.; Pant, D.; Breugelmans, T. The Inhibition of the Proton Donor Ability of Bicarbonate Promotes the Electrochemical Conversion of CO<sub>2</sub> in Bicarbonate Solutions. *Journal of CO<sub>2</sub> Utilization* **2021**, *48*, 101521. <https://doi.org/10.1016/j.jcou.2021.101521>.
- (25) Gutierrez-Sanchez, O.; Daems, N.; Bulut, M.; Deepak, P.; Breugelmans, T. Effects of Benzyl Functionalized Cationic Surfactants on the Inhibition of the Hydrogen Evolution Reaction in CO<sub>2</sub> Reduction Systems. *ACS Applied Materials & Interfaces* **2021**.

- (26) Li, T.; Lees, E. W.; Zhang, Z.; Berlinguette, C. P. Conversion of Bicarbonate to Formate in an Electrochemical Flow Reactor. *ACS Energy Letters* **2020**, *5* (8), 2624–2630. <https://doi.org/10.1021/acsenergylett.0c01291>.
- (27) Li, T.; Lees, E. W.; Goldman, M.; Salvatore, D. A.; Weekes, D. M.; Berlinguette, C. P. Electrolytic Conversion of Bicarbonate into CO in a Flow Cell. *Joule* **2019**, *3* (6), 1487–1497. <https://doi.org/10.1016/j.joule.2019.05.021>.
- (28) de Mot, B.; Hereijgers, J.; Daems, N.; Breugelmans, T. Insight in the Behavior of Bipolar Membrane Equipped Carbon Dioxide Electrolyzers at Low Electrolyte Flowrates. *Chemical Engineering Journal* **2022**, *428*, 131170. <https://doi.org/10.1016/j.cej.2021.131170>.
- (29) Vermaas, D. A.; Smith, W. A. Synergistic Electrochemical CO<sub>2</sub> Reduction and Water Oxidation with a Bipolar Membrane. *ACS Energy Letters* **2016**, *1* (6), 1143–1148. <https://doi.org/10.1021/acsenergylett.6b00557>.
- (30) Ramdin, M.; Morrison, A. R. T.; de Groen, M.; van Haperen, R.; de Kler, R.; van den Broeke, L. J. P.; Trusler, J. P. M.; de Jong, W.; Vlugt, T. J. H. High Pressure Electrochemical Reduction of CO<sub>2</sub> to Formic Acid/Formate: A Comparison between Bipolar Membranes and Cation Exchange Membranes. *Industrial & Engineering Chemistry Research* **2019**, *58* (5), 1834–1847. <https://doi.org/10.1021/acs.iecr.8b04944>.
- (31) Lees, E. W.; Goldman, M.; Fink, A. G.; Dvorak, D. J.; Salvatore, D. A.; Zhang, Z.; Loo, N. W. X.; Berlinguette, C. P. Electrodes Designed for Converting Bicarbonate into CO. *ACS Energy Letters* **2020**, 2165–2173. <https://doi.org/10.1021/acsenergylett.0c00898>.
- (32) Jouny, M.; Luc, W.; Jiao, F. General Techno-Economic Analysis of CO<sub>2</sub> Electrolysis Systems. *Industrial & Engineering Chemistry Research* **2018**, *57* (6), 2165–2177. <https://doi.org/10.1021/acs.iecr.7b03514>.
- (33) Ramdin, M.; Morrison, A. R. T.; de Groen, M.; van Haperen, R.; de Kler, R.; Irtem, E.; Laitinen, A. T.; van den Broeke, L. J. P.; Breugelmans, T.; Trusler, J. P. M.; Jong, W. de; Vlugt, T. J. H. High-Pressure Electrochemical Reduction of CO<sub>2</sub> to Formic Acid/Formate: Effect of PH on the Downstream Separation Process and Economics. *Industrial & Engineering Chemistry Research* **2019**, *58* (51), 22718–22740. <https://doi.org/10.1021/acs.iecr.9b03970>.

- (34) Jiang, J.; Wieckowski, A. Prospective Direct Formate Fuel Cell. *Electrochemistry Communications* **2012**, *18*, 41–43. <https://doi.org/10.1016/j.elecom.2012.02.017>.
- (35) An, L.; Chen, R. Direct Formate Fuel Cells: A Review. *Journal of Power Sources* **2016**, *320*, 127–139. <https://doi.org/10.1016/j.jpowsour.2016.04.082>.
- (36) Kortlever, R.; Tan, K. H.; Kwon, Y.; Koper, M. T. M. Electrochemical Carbon Dioxide and Bicarbonate Reduction on Copper in Weakly Alkaline Media. *Journal of Solid State Electrochemistry* **2013**, *17* (7), 1843–1849. <https://doi.org/10.1007/s10008-013-2100-9>.
- (37) Li, T.; Lees, E. W.; Zhang, Z.; Berlinguette, C. P. Conversion of Bicarbonate to Formate in an Electrochemical Flow Reactor. *ACS Energy Letters* **2020**, *5* (8), 2624–2630. <https://doi.org/10.1021/acseenergylett.0c01291>.
- (38) de Mot, B.; Hereijgers, J.; Duarte, M.; Breugelmans, T. Influence of Flow and Pressure Distribution inside a Gas Diffusion Electrode on the Performance of a Flow-by CO<sub>2</sub> Electrolyzer. *Chemical Engineering Journal* **2019**, *378*, 122224. <https://doi.org/10.1016/j.cej.2019.122224>.
- (39) Akbashev, A. R. Electrocatalysis Goes Nuts. *ACS Catalysis* **2022**, 4296–4301. <https://doi.org/10.1021/acscatal.2c00123>.
- (40) del Castillo, A.; Alvarez-Guerra, M.; Solla-Gullón, J.; Sáez, A.; Montiel, V.; Irabien, A. Electrocatalytic Reduction of CO<sub>2</sub> to Formate Using Particulate Sn Electrodes: Effect of Metal Loading and Particle Size. *Applied Energy* **2015**, *157*, 165–173. <https://doi.org/10.1016/j.apenergy.2015.08.012>.
- (41) de Mot, B.; Ramdin, M.; Hereijgers, J.; Vlugt, T. J. H.; Breugelmans, T. Direct Water Injection in Catholyte-Free Zero-Gap Carbon Dioxide Electrolyzers. *ChemElectroChem* **2020**, *7* (18), 3839–3843. <https://doi.org/10.1002/celc.202000961>.
- (42) Liu, H.; Miao, B.; Chuai, H.; Chen, X.; Zhang, S.; Ma, X. Nanoporous Tin Oxides for Efficient Electrochemical CO<sub>2</sub> Reduction to Formate. *Green Chemical Engineering* **2021**. <https://doi.org/10.1016/j.gce.2021.11.001>.
- (43) Al-Tamreh, S. A.; Ibrahim, M. H.; El-Naas, M. H.; Vaes, J.; Pant, D.; Benamor, A.; Amhamed, A. Electroreduction of Carbon Dioxide into Formate: A Comprehensive Review. *ChemElectroChem* **2021**, *8* (17), 3207–3220. <https://doi.org/10.1002/celc.202100438>.

- (44) Damas, G. B.; Miranda, C. R.; Sgarbi, R.; Portela, J. M.; Camilo, M. R.; Lima, F. H. B.; Araujo, C. M. On the Mechanism of Carbon Dioxide Reduction on Sn-Based Electrodes: Insights into the Role of Oxide Surfaces. *Catalysts* **2019**, *9* (8), 636. <https://doi.org/10.3390/catal9080636>.
- (45) Baruch, M. F.; Pander, J. E.; White, J. L.; Bocarsly, A. B. Mechanistic Insights into the Reduction of CO<sub>2</sub> on Tin Electrodes Using in Situ ATR-IR Spectroscopy. *ACS Catalysis* **2015**, *5* (5), 3148–3156. <https://doi.org/10.1021/acscatal.5b00402>.
- (46) Merino-Garcia, I.; Tinat, L.; Albo, J.; Alvarez-Guerra, M.; Irabien, A.; Durupthy, O.; Vivier, V.; Sánchez-Sánchez, C. M. Continuous Electroconversion of CO<sub>2</sub> into Formate Using 2 Nm Tin Oxide Nanoparticles. *Applied Catalysis B: Environmental* **2021**, *297*, 120447. <https://doi.org/10.1016/j.apcatb.2021.120447>.
- (47) Kutz, R. B.; Chen, Q.; Yang, H.; Sajjad, S. D.; Liu, Z.; Masel, I. R. Sustainion Imidazolium-Functionalized Polymers for Carbon Dioxide Electrolysis. *Energy Technology* **2017**, *5* (6), 929–936. <https://doi.org/10.1002/ente.201600636>.
- (48) Li, C. W.; Kanan, M. W. CO<sub>2</sub> Reduction at Low Overpotential on Cu Electrodes Resulting from the Reduction of Thick Cu<sub>2</sub>O Films. *J Am Chem Soc* **2012**, *134* (17), 7231–7234. <https://doi.org/10.1021/ja3010978>.
- (49) Feaster, J. T.; Shi, C.; Cave, E. R.; Hatsukade, T.; Abram, D. N.; Kuhl, K. P.; Hahn, C.; Nørskov, J. K.; Jaramillo, T. F. Understanding Selectivity for the Electrochemical Reduction of Carbon Dioxide to Formic Acid and Carbon Monoxide on Metal Electrodes. *ACS Catalysis* **2017**, *7* (7), 4822–4827. <https://doi.org/10.1021/acscatal.7b00687>.
- (50) Oloman, C.; Li, H. Electrochemical Processing of Carbon Dioxide. *ChemSusChem* **2008**, *1* (5), 385–391. <https://doi.org/10.1002/cssc.200800015>.
- (51) Li, Y. C.; Yan, Z.; Hitt, J.; Wycisk, R.; Pintauro, P. N.; Mallouk, T. E. Bipolar Membranes Inhibit Product Crossover in CO<sub>2</sub> Electrolysis Cells. *Advanced Sustainable Systems* **2018**, *1700187*, 1700187. <https://doi.org/10.1002/adsu.201700187>.
- (52) Wang, N.; Miao, R. K.; Lee, G.; Vomiero, A.; Sinton, D.; Ip, A. H.; Liang, H.; Sargent, E. H. Suppressing the Liquid Product Crossover in Electrochemical CO<sub>2</sub> Reduction. *SmartMat* **2021**, *2* (1), 12–16. <https://doi.org/10.1002/smm2.1018>.
- (53) Bourcier, W. L.; Stolaroff, J. K.; Smith, M. M.; Aines, R. D. Achieving Supercritical Fluid CO<sub>2</sub> Pressures Directly from Thermal Decomposition of Solid Sodium Bicarbonate.

- Energy Procedia* **2017**, *114*, 2545–2551.  
<https://doi.org/10.1016/j.egypro.2017.03.1412>.
- (54) Blommaert, M. A.; Aili, D.; Tufa, R. A.; Li, Q.; Smith, W. A.; Vermaas, D. A. Insights and Challenges for Applying Bipolar Membranes in Advanced Electrochemical Energy Systems. *ACS Energy Letters* **2021**, *6* (7), 2539–2548.  
<https://doi.org/10.1021/acsenergylett.1c00618>.
- (55) Franzen, D.; Ellendorff, B.; Paulisch, M. C.; Hilger, A.; Osenberg, M.; Manke, I.; Turek, T. Influence of Binder Content in Silver-Based Gas Diffusion Electrodes on Pore System and Electrochemical Performance. *Journal of Applied Electrochemistry* **2019**, *49* (7), 705–713. <https://doi.org/10.1007/s10800-019-01311-4>.
- (56) Arinton, G.; Rianto, A.; Faizal, F.; Hidayat, D.; Hidayat, S.; Panatarani, C.; Joni, I. M. Effect of Binders on Natural Graphite Powder-Based Gas Diffusion Electrode for Mg-Air Cell; 2016; p 030055. <https://doi.org/10.1063/1.4943750>.

## Table of contents

